

A heptameric peptide purified from *Spirulina* sp. gastrointestinal hydrolysate inhibits angiotensin I-converting enzyme- and angiotensin II-induced vascular dysfunction in human endothelial cells

SEONG-YEONG HEO^{1,2*}, SEOK-CHUN KO^{1,2*}, CHANG SU KIM^{3*}, GUN-WOO OH^{1,2}, BOMI RYU⁴, ZHONG-JI QIAN⁵, GEUNHYUNG KIM⁶, WON SUN PARK⁷, IL-WHAN CHOI⁸, THI TUONG VY PHAN^{1,2}, SOO-JIN HEO⁹, DO-HYUNG KANG⁹, MYUNGGI YI^{1,2} and WON-KYO JUNG^{1,2}

¹Department of Biomedical Engineering, and Center for Marine-Integrated Biomedical Technology (BK21 Plus) and ²Marine-Integrated Bionics Research Center, Pukyong National University, Busan 48513; ³Department of Orthopedic Surgery, Kosin University Gospel Hospital, Busan 49267, Republic of Korea; ⁴School of Pharmacy, The University of Queensland, Brisbane, QLD 4072, Australia; ⁵College of Food Science and Technology, Guangdong Ocean University, Zhanjiang, Guangdong 524088, P.R. China; ⁶Department of Bio-Mechatronic Engineering, College of Biotechnology and Bioengineering, Sungkyunkwan University, Suwon, Gyeonggi 16419; ⁷Department of Physiology, Kangwon National University, School of Medicine, Chuncheon, Gangwon 24341; ⁸Department of Microbiology, Inje University College of Medicine, Busan 47392; ⁹Jeju International Marine Science Center for Research and Education, Korea Institute of Ocean Science and Technology (KIOST), Jeju 63349, Republic of Korea

Received June 4, 2016; Accepted March 13, 2017

DOI: 10.3892/ijmm.2017.2941

Abstract. In this study, a marine microalga *Spirulina* sp.-derived protein was hydrolyzed using gastrointestinal enzymes to produce an angiotensin I (Ang I)-converting enzyme (ACE) inhibitory peptide. Following consecutive purification, the potent ACE inhibitory peptide was composed of 7 amino acids, Thr-Met-Glu-Pro-Gly-Lys-Pro (molecular weight, 759 Da). Analysis using the Lineweaver-Burk plot and molecular modeling suggested that the purified peptide acted as a mixed non-competitive inhibitor of ACE. The inhibitory effects of

the peptide against the cellular production of vascular dysfunction-related factors induced by Ang II were also investigated. In human endothelial cells, the Ang II-induced production of nitric oxide and reactive oxygen species was inhibited, and the expression of inducible nitric oxide synthase (iNOS) and endothelin-1 (ET-1) was downregulated when the cells were cultured with the purified peptide. Moreover, the peptide blocked the activation of p38 mitogen-activated protein kinase. These results indicated that this *Spirulina* sp.-derived peptide warrants further investigation as a potential pharmacological inhibitor of ACE and vascular dysfunction.

Correspondence to: Professor Myunggi Yi or Professor Won-Kyo Jung, Department of Biomedical Engineering, and Center for Marine-Integrated Biomedical Technology (BK21 Plus), Pukyong National University, 45 Yongso-ro, Busan 48513, Republic of Korea
E-mail: myunggi@pknu.ac.kr
E-mail: wkjung@pknu.ac.kr

*Contributed equally

Abbreviations: ACE, angiotensin I-converting enzyme; Ang, angiotensin; NO, nitric oxide; ROS, reactive oxygen species; ET-1, endothelin-1; iNOS, inducible nitric oxide synthase; MAPKs, mitogen-activated protein kinases

Key words: *Spirulina* sp., angiotensin I-converting enzyme, angiotensin II, vascular dysfunction, mitogen-activated protein kinases

Introduction

Hypertension is a condition of major concern for health care that markedly increases the risk of death from stroke, myocardial infarction, arteriosclerosis, cerebral hemorrhage and other vascular diseases (1). The renin-angiotensin system is an endogenous regulator of blood pressure, water electrolyte homeostasis and cell growth balance (2). In particular, it plays a key role in the pathology of hypertension (3). In the renin-angiotensin system, angiotensin I (Ang I)-converting enzyme (ACE) hydrolyzes the inactive decapeptide Ang I by cleaving a dipeptide from the C-terminus to produce the potent vasoconstrictor Ang II, which is responsible for increasing arterial pressure (4,5). Therefore, the modulation of the renin-angiotensin system has become a promising approach for controlling blood pressure in the treatment of cardiovascular

disorders, for example by using ACE inhibitors as therapeutic agents.

Many synthetic ACE inhibitors have been used extensively in the treatment of hypertension and cardiovascular disorders; these inhibitors include the drugs captopril, enalapril, alacepril and lisinopril (6,7). However, they have been reported to have some side-effects, including coughing, a disrupted sense of taste, azotemia, angioedema and skin rashes (7). Therefore, ACE inhibitors from natural sources are currently being considered as alternative therapeutic agents for controlling blood pressure (2-4,6,7).

Ang II has pleiotropic acute and chronic effects on vascular smooth muscle and plays an important role in cardiovascular diseases, including hypertension, atherosclerosis and heart failure (8,9). In this regard, it has been suggested that Ang II induces the production of other vascular dysfunction-related factors, such as free radicals [nitric oxide (NO) and reactive oxygen species (ROS)] and vasoconstrictors [endothelin-1 (ET-1) and vasopressin] (10-12). These factors can promote cellular oxidative stress and induce vascular endothelial dysfunction, hypertension and atherosclerosis (11). Therefore, research into ACE inhibitors has focused on decreasing the production of Ang II to control the systemic balance between the potent vasoactive regulators, ET-1 and free radicals.

Microalgae contain various valuable natural compounds, such as pigments, β -carotenes, polysaccharides and peptides that have uses in the pharmaceutical, cosmetic and nutraceutical industries (13,14). Therefore, microalgae are potentially an excellent source of natural compounds that may be used as ingredients for preparing functional foods and nutraceuticals. Although microalgae possess >50% protein in their biomass, they are usually used as animal feed (6). However, microalgal proteins can be converted into value-added products with improved functional properties by enzymatic hydrolysis. As a result, researchers are interested in obtaining effective bioactive peptides from marine microalgae (13,15-17).

Among the microalgae, *Spirulina* is a blue-green alga appertaining to the Oscillatoraceae family. It is grown in marine and freshwater environments and is referred to as a 'superfood' which has several biological activities, such as antioxidant, anti-diabetic, cholesterol-controlling and insulin resistance effects (18). Although, Suetsuna and Chen reported thye anti-hypertensive effect of *Spirulina* (16), no study to date has shown an inhibitory effect of *Spirulina* on Ang II-induced endothelial dysfunction, at least to the best of our knowledge.

The principal objective of the present study was to purify and identify an ACE inhibitory peptide from *Spirulina* sp., and to determine the mechanisms underlying the effects of the purified peptide on ACE and on the production of vascular dysfunction-related factors by Ang II-stimulated human endothelial cells.

Materials and methods

Materials. ACE (from rabbit lung), N-Hippuryl-His-Leu tetrahydrate (HHL), Griess reagent, 3-(4,5-dimethylthiazol-2-yl)-2,5-diphenyltetrazolium bromide (MTT), gastrointestinal enzymes (pepsin, α -chymotrypsin and trypsin) and Ang II were all purchased from Sigma-Aldrich (St. Louis, MO, USA). Specific antibodies against inducible nitric oxide synthase (iNOS; sc-7271), GAPDH (sc-25778), p-p38

(sc-7973), p38 (sc-7149), p-c-Jun N-terminal kinase (JNK; sc-6254), JNK (sc-7345), p-extracellular signal-regulated kinase (ERK; sc-7383), ERK (sc-292838) and ET-1 (sc-21625) were all purchased from Santa Cruz Biotechnology, Inc. (Santa Cruz, CA, USA), and 2',7'-dichlorodihydrofluorescein diacetate (DCFH-DA) and Hoechst 33342 were obtained from Invitrogen Life Technologies (Carlsbad, CA, USA). The HiPrep™ 16/10 DEAE FF anion exchange column was purchased from GE Healthcare (Buckinghamshire, UK). The other chemicals and reagents were of analytical grade.

Preparation of enzymatic hydrolysate of marine microalga, *Spirulina* sp. The enzymatic hydrolysis of the marine microalga, *Spirulina* sp., was performed using gastrointestinal enzymes, as previously described (19). A total of 100 ml of 4% (w/v) *Spirulina* sp. solution was brought to pH 2.2 in gastric digestion using HCl or NaOH under rigorous mixing. Pepsin (EC 3.4.23.1) was added at the enzyme to substrate ratio of 1/100 (w/w), followed by incubation at 37°C on a shaker for 2 h. The pH was set to 6.5 to obtain the conditions of small intestinal digestion. Trypsin (EC 3.4.21.4) and α -chymotrypsin (EC 3.4.21.1) were both supplemented at an enzyme to substrate ratio of 1/100 (w/w), then incubated at 37°C for 2.5 h. The hydrolysate was then boiled for 10 min at 100°C to inactivate the enzyme reaction. The collected sample was clarified by centrifugation (10,000 x g for 15 min at 4°C) for removal of the residue. The hydrolysate was passed through ultrafiltration (UF) membranes [molecular weight (MW) cut-off of 5, 10 and 100 kDa] using Millipore's UF system (Millipore, Bedford, MA, USA). The gastrointestinal hydrolysate was subjected to molecular weight fractionation to obtain the peptide with a molecular weight of <5 kDa (5 kDa or smaller), 5-10 kDa (between 5 and 10 kDa), 10-100 kDa (between 10 and 100 kDa) and >100 kDa (100 kDa and larger). All recovered fractions were lyophilized and store -80°C until use.

Purification of ACE inhibitory peptide. The highest ACE inhibitory fraction was loaded onto an HiPrep DEAE FF ion-exchange column using fast protein liquid chromatography (FPLC ÄKTA; Amersham Biosciences, Uppsala, Sweden). The column was equilibrated in 20 mM sodium phosphate buffer (pH 7.0) previously, and eluted with a linear gradient of NaCl (0-2 M) at a flow rate of 2 ml/min. Elution peaks were monitored at 280 nm. The fractions were further purified on a PrimeSphere ODS C₁₈ column permeation reversed-phase high-performance liquid chromatography (RP-HPLC) with a linear gradient of acetonitrile (0-35% in 35 min) containing 0.1% trifluoroacetic acid (TFA) at a flow rate of 0.8 ml/min. Finally, the fraction with the ACE inhibitory activity was collected and lyophilized; this was followed by identification of the amino acid sequence.

Determination of molecular weight and amino acid sequence. An accurate molecular mass and amino acid sequence of the purified peptide was determined using a quadrupole time-of-flight mass spectroscopy (Micromass, Altrincham, UK) coupled with an electrospray ionization (ESI) source. The purified peptide was separately infused into the electrospray source after being dissolved in methanol/water (1:1, v/v), and the molecular mass was determined by the doubly charged [M+2H]²⁺ state in the mass spectrum. Following molecular

mass determination, the peptide was automatically selected for fragmentation, and sequence information was obtained by tandem MS analysis.

Measurement of ACE inhibitory activity. The ACE inhibitory activity assay was performed according to the method of Cushman and Cheung (20) with slight modifications. For each assay, 50 μ l of the hydrolysate solution with 50 μ l of ACE solution (25 mU/ml) was pre-incubated at 37°C for 30 min, and then incubated with 100 μ l of substrate (25 mM HHL in 50 mM sodium borate buffer at pH 8.3) at 37°C for 60 min. The reaction was terminated by the addition of 250 μ l of 1 N HCl. Hippuric acid was extracted with 500 μ l of ethyl acetate. Subsequently, a 200 μ l aliquot of the extract was removed by evaporation in a dry oven at 80°C. The residue was dissolved in 1 ml distilled water and its UV spectra density was measured at 228 nm using a microplate reader (PowerWave XS2; BioTek Instruments, Inc., Winooski, VT, USA).

Determination of ACE inhibition pattern. Various concentrations of ACE inhibitory peptide were added to each reaction mixture, as previously described by Bush *et al* (21). The enzyme activity was measured with various concentrations of the substrate. The ACE inhibitory pattern in the presence of the inhibitor was obtained by the Lineweaver-Burk plots.

Molecular modeling. In order to find the binding site of the purified peptide and to understand the mixed non-competitive inhibition mechanism further, a three-stage molecular modeling was carried out by Monte Carlo (MC) and molecular dynamics (MD) simulations. The simulation system was composed of ACE, Ang II and the purified peptide. The crystal structure of ACE in complex with Ang II (PDB ID, 4APH) was used to set up the system. Ang II is the principal end-product of the enzyme function. Since the purified peptide is a mixed non-competitive inhibitor, Ang II was kept in the docking simulation system to avoid overlapping between the binding site of the purified peptide and the binding site of the substrate. Ang II shares the binding site with Ang I, the substrate of the enzyme.

In the first stage, docking of the purified peptide around the ACE complex was performed, and the resulting model structures were then clustered based on the location and the orientation of the peptide relative to the ACE complex. In four clusters, we selected the structure with the lowest score of each cluster to run the second stage of docking for further sampling. In the final stage, MD simulation was carried out using the structure with the lowest score of the models generated in the second stage in order to relax the structure further with explicit water molecules.

Docking simulations. The binding site of the purified peptide on the ACE complex was searched by docking simulations using the FlexPepDock protocol in the Rosetta program, which is designed for modeling complexes between a flexible peptide and a globular protein (22). Using the MC with minimization approach in the main part of FlexPepDock protocol (22), backbone torsion angles and rigid body orientations of the peptide were optimized relative to the protein. In the first stage of docking, 555 simulations were performed with different initial positions and orientations of the peptide around the ACE protein to cover the inside and the outside of the cleft of two sub domains. The lowest energy scores of each docking resulting

111,000 model structures simulation on the outside of the cleft were higher than those on the inside of the cleft. Based on the location and the orientation of the purified peptide inside the cleft, resulting docking structures were categorized into four clusters. The structure with the lowest score of each cluster was selected, and the second stage of the docking simulations was carried out with these four initial conformations of the peptide. Using the 4 models with the lowest score of each cluster as initial structures, the second stage of docking simulations were carried out to sample 8,000 models further.

MD simulation. The structure of the complex of ACE, Ang II and the purified peptide with the lowest score of the second stage of docking simulations was selected to run MD simulation. The complex system was solvated in a truncated octahedral box with 23,410 TIP3P water molecules (23) and 0.1 M NaCl ions. All MD simulations were carried out using NAMD software (24) with CHARMM force field (25) under the periodic boundary condition. After removing bad contacts with 1,000 steps of energy minimization, the MD simulation began by gradually heating up the system from 10 to 310 K for 60 psec under the constant volume condition. Afterward, all simulation was switched to constant temperature and pressure conditions (NPT). The simulation system was equilibrated for 200 psec. All C α atoms in the steps of energy minimization, heating and equilibration were restrained with harmonic constant 1 kcal/mol \cdot A 2 , and the following MD simulation was continued without any restraint. All bonds involving hydrogen atoms were constrained, allowing an integration time step of 2 fsec, and the average pressure and temperature were maintained at 1 bar and 310 K. The non-bonded interactions (Van der Waals and electrostatic interactions) were smoothly truncated from 10 to 12 Å cut-off, and the particle-mesh Ewald method was used to treat long-range electrostatic interactions (26). The simulation system was stabilized at 36.57 nsec, and the total length of MD simulation was 123.83 nsec. The trajectory from 36.57 to 123.83 nsec, the end of the simulation time, was analyzed in the study.

Cell culture analysis of the purified peptide

Cell culture and cell viability. Human umbilical vein endothelial cells (EA.hy926) were kindly provided by Professor S.K. Kim from Pukyong National University, Busan, Korea. The cells were cultured in Dulbecco's modified Eagle's medium (DMEM) supplemented with 10% fetal bovine serum (FBS), penicillin (100 U/ml) and streptomycin (100 μ g/ml) at 37°C in 5% CO $_2$ humidified air environment.

Cytotoxic assessment by MTT assay. Cell viability was determined by MTT reduction assay. The EA.hy926 cells were plated on 96-well plates, which were pre-incubated and subsequently treated with Ang II (1 μ M) coupled with aliquots of the purified peptide (62.5, 125 and 250 μ M) at 37°C for 24 h. MTT stock solution was then added to each well. Following incubation for 4 h, the plates were centrifuged (800 x g, 5 min), and the supernatants were aspirated. The formazan crystals in each well were dissolved in DMSO, and the absorbance was measured using a microplate reader (PowerWave XS2; BioTek Instruments, Inc.) at 540 nm.

Determination of NO and ROS levels. NO levels in the culture supernatants were determined by measuring nitrite, which is a major stable product of NO, using Griess reagent. Following

the pre-incubation of the EA.hy926 cells with the purified peptide and Ang II for 24 h, the quantity of nitrite which had accumulated in the culture medium was measured as an indicator of NO production. Briefly, a 100 μ l of cell culture medium was mixed with 100 μ l of Griess reagent (1% sulfanilamide and 0.1% naphthylethylenediamine dihydrochloride in 2.5% phosphoric acid), the mixture was incubated at room temperature for 10 min, and the absorbance at 540 nm was measured using a microplate reader. Fresh culture medium was used as a blank in every experiment.

The intracellular generation of ROS was then detected by oxidation of the cell permeable fluorescence dye 5-(and-6)-carboxy-2',7'-dichlorofluorescein diacetate (carboxy-DCFH-DA) to the fluorescent DCF by Ang II. The EA.hy926 cells were seeded on 24-well plate. After 24 h, the cells were pre-treated with various concentrations of the purified peptide. After 30 min, Ang II was added at a concentration of 1 μ M, and the cells were then incubated for an additional 30 min at 37°C under a humidified atmosphere. Finally, 40 μ M carboxy-DCFH-DA was introduced to the cells, and carboxy-DCFH-DA and DAPI was imaged using a fluorescence microscope (Axio Observer A1; Zeiss, Jena, Germany).

Western blot analysis. The cells were lysed in lysis buffer (20 mM Tris, 5 mM EDTA, 10 mM $\text{Na}_4\text{P}_2\text{O}_7$, 100 mM NaF, 2 mM Na_3VO_4 , 1% NP-40, 10 mg/ml aprotinin, 10 mg/ml leupeptin and 1 mM PMSF) for 60 min and then centrifuged at 12,000 rpm and 4°C for 15 min. The protein concentrations were determined using the BCA™ protein assay kit. The lysate containing 40 μ g of protein was subjected to electrophoresis on a sodium dodecyl sulfate (SDS)-polyacrylamide gel, and the gel was transferred onto nitrocellulose membranes. The membranes were blocked with 5% non-fat dry milk in TBS-T (25 mM Tris-HCl, 137 mM NaCl, 2.65 mM KCl and 0.05% Tween-20, pH 7.4) for 2 h. The primary antibodies were used at a 1:1,000 dilution. The membranes were incubated with the primary antibodies at 4°C overnight, washed with TBS-T and then incubated with the secondary antibodies (G21040 and G21234; Invitrogen Life Technologies) at 1:3,000 dilutions. The signals were developed using an ECL western blotting detection kit and quantified using an LAS3200® luminescent image analyzer and protein expression was quantified by Multi Gauge V3.0 software (Fujifilm Life Science, Tokyo, Japan).

Statistical analysis. All quantitative data are presented as the means \pm standard deviation (SD) with least 3 individual experiments that were conducted using fresh reagents. Significant differences between the groups were determined using the unpaired Student's t-test. The differences were considered statistically significant at $P < 0.05$.

Results

Fractionation of *Spirulina* sp. protein hydrolysate to produce an ACE inhibitory peptide. *Spirulina* was hydrolyzed using gastrointestinal enzymes that increase the absorption of active peptides, including pepsin, α -chymotrypsin and trypsin, under simulated physiological conditions. The obtained hydrolysate was tested for its potential to inhibit ACE. In the ACE inhibitory assay (Table I), the hydrolysate IC_{50} value was

Table I. ACE inhibitory activity of molecular weight fractions from gastrointestinal hydrolysate of *Spirulina* sp.

Fraction	IC_{50} value (mg/ml) ^a
Unfractionated ^b	0.98 \pm 0.02
>100 kDa ^c	1.06 \pm 0.03
10-100 kDa	0.96 \pm 0.02
5-10 kDa	0.97 \pm 0.01
<5 kDa	0.66 \pm 0.03

The values of IC_{50} were determined by at triplicate individual experiments. ^aThe concentration of an inhibitor required to inhibit 50% of ACE activity. ^bGastrointestinal hydrolysate. ^cUF membrane (molecular weight cut-off 5, 10 and 100 kDa) was used. ACE, angiotensin I-converting enzyme.

Table II. Purification of ACE inhibitory peptide of gastrointestinal hydrolysate from *Spirulina* sp.

Purification step	IC_{50} value (mg/ml) ^a	Purification fold
Gastrointestinal hydrolysate	0.98 \pm 0.02	1
Ultrafiltration (<5 kDa)	0.66 \pm 0.03	1.48
FPLC ^b	0.30 \pm 0.01	2.97
RP-HPLC ^c	0.10 \pm 0.02	9.80

The values of IC_{50} were determined by at triplicate individual experiments. ^aThe concentration of an inhibitor required to inhibit 50% of ACE activity. ^bFast protein liquid chromatography. ^cReversed-phase high-performance liquid chromatography. ACE, angiotensin I-converting enzyme.

exhibited by the gastrointestinal hydrolysate of *Spirulina* sp. at 0.98 mg/ml. The hydrolysate was fractionated using an ultrafiltration membrane system into 4 individual fractions with MWs of <5, 5-10, 10-100 and >100 kDa, respectively, and the resultant fractions were also analyzed for their abilities to inhibit ACE. Among all the MW groups, the <5 kDa fraction exhibited the highest ACE inhibitory activity and had an IC_{50} value of 0.66 mg/ml (Table I). Therefore, we selected the <5 kDa fraction for further purification of an ACE inhibitory peptide.

Purification of ACE inhibitory peptide. An ACE inhibitory peptide was purified from the marine *Spirulina* sp. by using chromatographic methods, combining FPLC on a HiPrep™ DEAE FF 16/10 anion-exchange column (GE Healthcare). As shown in Fig. 1A, there were 4 major absorbance peaks at 280 nm and 5 fractions associated with the peaks were pooled and lyophilized for ACE inhibitory activity. Among the fractions, fraction Fr5 exhibited the strongest ACE inhibitory activity and had an IC_{50} value of 0.3 mg/ml (Fig. 1B). The active fraction was further separated by RP-HPLC on a PrimeSphere™ ODS column (Phenomenex, Torrance, CA, USA) with a linear gradient of acetonitrile (0-35% for 35 min) containing 0.1% TFA. The elution profiles of the

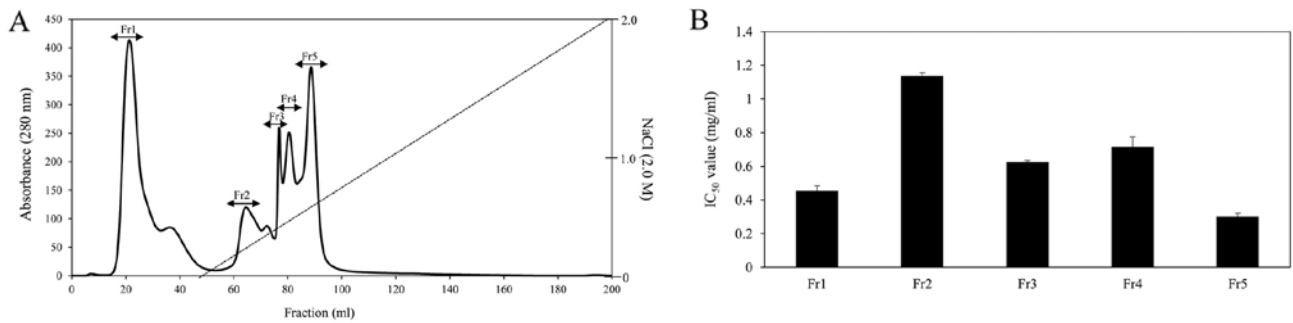


Figure 1. (A) Fast protein liquid chromatography (FPLC) of tryptic hydrolysate loaded (2 ml) onto a HiPrep™ 16/10 DEAE FF anion-exchange column. (B) ACE inhibitory activity of each fraction from FPLC.

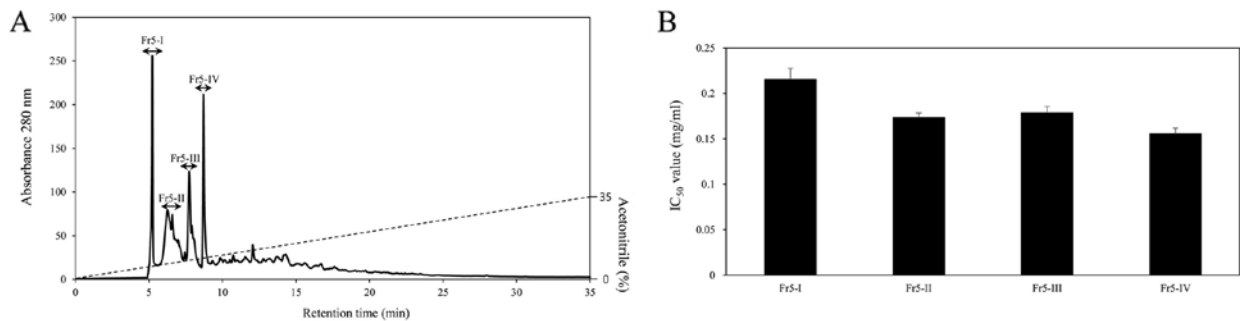


Figure 2. (A) Reversed-phase high-performance liquid chromatography (RP-HPLC) chromatogram of the potent angiotensin I (Ang I)-converting enzyme (ACE) inhibitory activity fraction isolated from fast protein liquid chromatography (FPLC). (B) ACE inhibitory activity of each fraction from RP-HPLC.

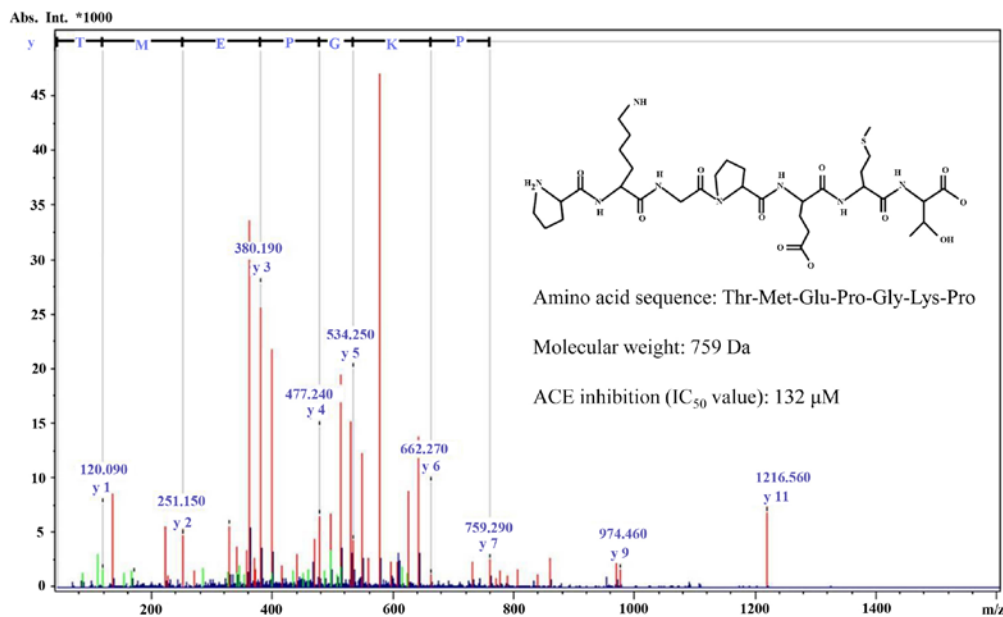


Figure 3. Identification of the molecular mass and amino acid sequence of the angiotensin I (Ang I)-converting enzyme (ACE) inhibition peptide using quadrupole time-of-flight mass spectrometry with an electrospray ionization (ESI) source.

peaks are shown in Fig. 2A. The peaks were separated into 4 peaks (Fr5-I to Fr5-IV) and each peak was pooled for ACE inhibitory activity. The Fr5-IV peak exhibited the most potent ACE inhibitory activity, with an IC_{50} value of 0.1 mg/ml (Fig. 2B). The typical results investigated during the purification processes are summarized in Table II. The ACE inhibitory peptide was purified 10.2-fold from the enzymatic hydrolysate using a 3-step purification procedure.

The molecular mass of the purified ACE inhibitory peptide was determined to be 759 Da by quadrupole time-of-flight mass spectrometry coupled to an electrospray ionization source. Its full amino acid sequence was determined to be Thr-Met-Glu-Pro-Gly-Lys-Pro (Fig. 3).

ACE inhibition pattern and molecular modeling of the purified ACE inhibitory peptide. The ACE inhibition pattern of the

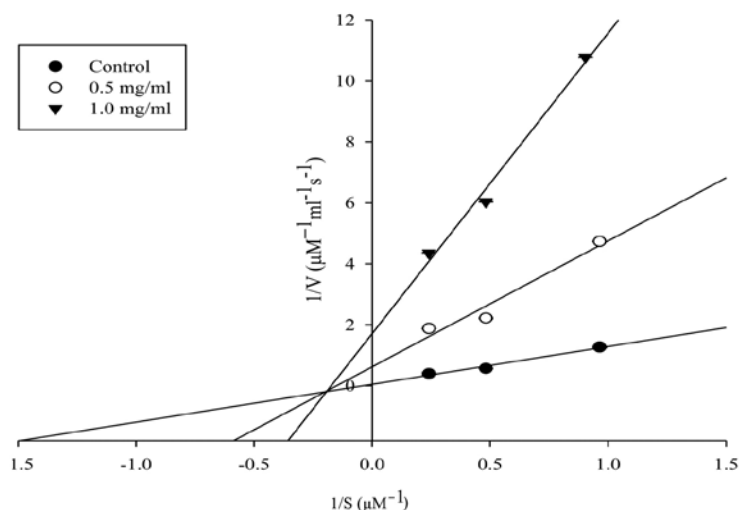


Figure 4. Lineweaver-Burk plots for determination of inhibitory mode of purified peptide on angiotensin I (Ang I)-converting enzyme (ACE). ACE inhibitory activity was determined in the presence or absence of purified peptide as described in the text using N-Hippuryl-His-Leu tetrahydrate (HHL) as the enzyme substrate.

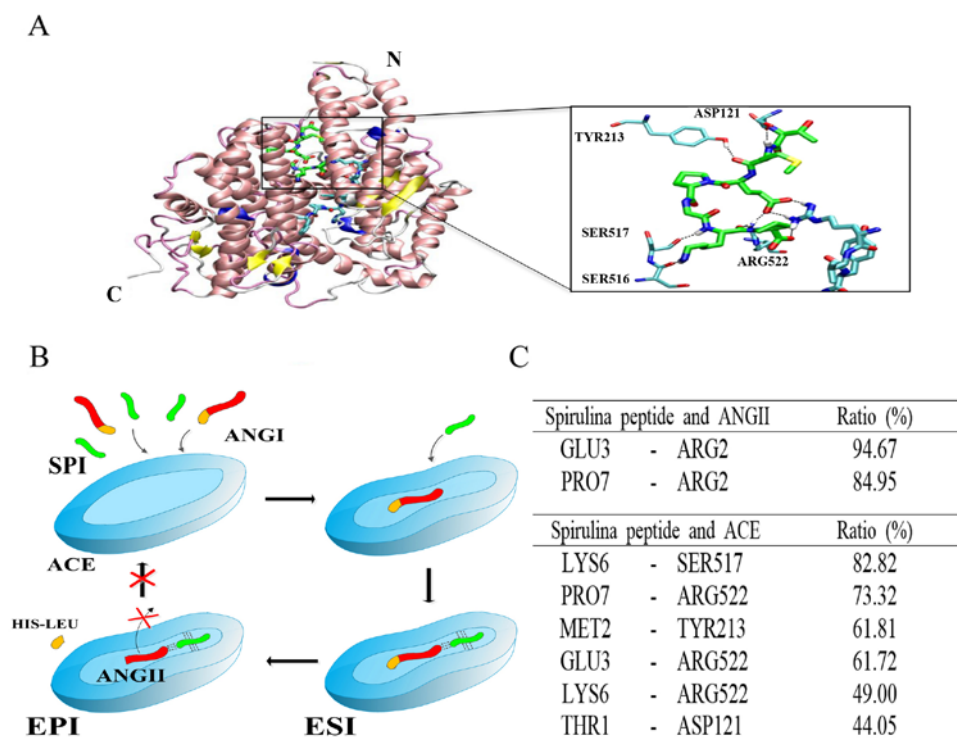


Figure 5. The binding site of the purified peptide in the cleft of ACE. ACE is represented by ribbons, and zinc atom in active site is represented by a gray sphere. Ang II and the purified peptide are represented by thick sticks, and amino acids of ACE involved in hydrogen bonds are represented by thin sticks. (A) Carbon, nitrogen, oxygen, sulfur and hydrogen atoms are colored by cyan, blue, red, yellow and white, respectively. Carbon atoms of the purified peptide are colored by green. N and C indicate the N- and C-terminus of the enzyme, respectively. The snapshot is taken at 121.6 nsec. (B) Mixed non-competitive inhibition mechanism of ACE by the purified peptide. The broken lines indicate hydrogen bonds (I, inhibitor, or the purified peptide; ACE, angiotensin I-converting enzyme; Ang I, angiotensin I, or substrate; Ang II, angiotensin II, or product; ESI, enzyme-substrate-inhibitor complex; EPI, enzyme-product-inhibitor complex, dead-end complex). (C) Ratio of the presence of hydrogen bond pairs during the simulation time.

purified peptide was investigated by Lineweaver-Burk plots and was found to show a mixed non-competitive inhibition pattern (Fig. 4). Moreover, based on molecular modeling, we were able to determine a mixed non-competitive inhibition mechanism of ACE by the purified peptide (Fig. 5). The ACE binding site of the purified peptide was predicted by 3-stage molecular modeling. The peptide bound in the N-terminal side of the cleft formed by two sub-domains of ACE and next to

the binding site of Ang II (Fig. 5A and B). The binding of the purified peptide was stabilized by hydrogen bond interactions with ACE and Ang II. We investigated the presence of hydrogen bonds by performing MD simulations using a distance of 3.4 Å and a rotation angle of 30°. On average, during MD simulation, the purified peptide formed 5.76 ± 1.50 and 2.58 ± 0.83 pairs of hydrogen bonds with ACE and Ang II, respectively, at the same time (data expressed as the means \pm SD). The most frequently

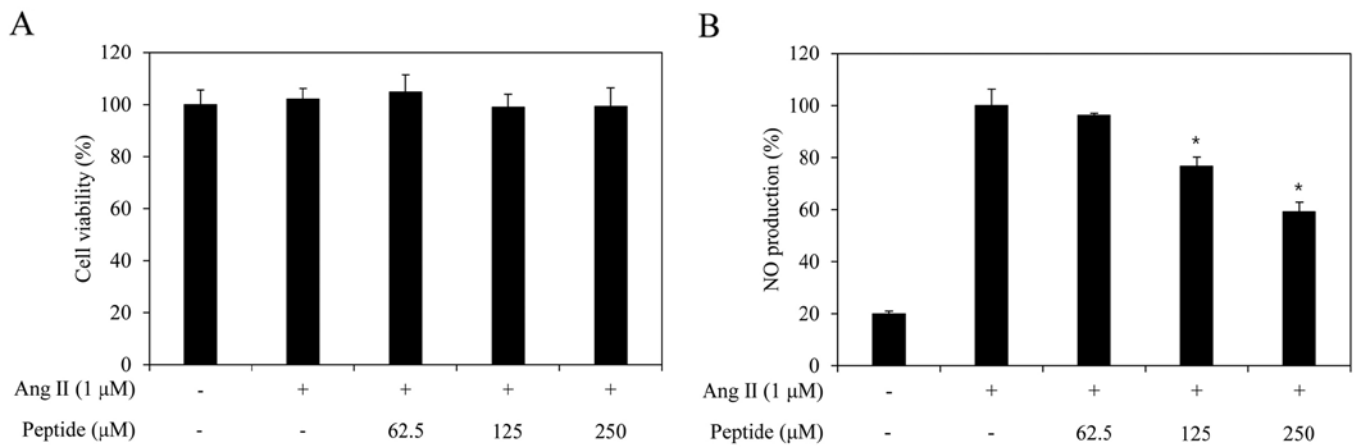


Figure 6. (A) Effect of peptide on cell viability and (B) nitric oxide (NO) production in angiotensin II (Ang II)-stimulated Ea.hy926 cells. The cells were pre-treated for 1 h with various concentrations (62.5, 125 and 250 μ M) of the purified peptide. Ang II (1 μ M) was then added, and the cells were incubated for 24 h. The cytotoxicity was determined by MTT assay. * $p < 0.05$ indicate significant differences compared with the Ang II-stimulated group.

formed pairs of hydrogen bonds during the MD simulation are listed in Fig. 5C. In addition to hydrogen bonds, binding of the peptide was stabilized by van der Waals interactions. The MD simulation results revealed that Pro4 of the purified peptide was bound in the hydrophobic pocket formed by Ile204, Ala208 and Trp220 of ACE. This result indicates that the purified peptide can combine with ACE to produce a dead-end complex, regardless of whether a substrate molecule is bound or not. Thus, the purified peptide must be bound to an alternative site of the enzyme. Taken together, the results suggest that the peptide acts as an ACE inhibitor by forming enzyme-substrate-inhibitor and enzyme-inhibitor complexes to suppress the catalytic activity of ACE.

Cytotoxicity of the purified peptide and its inhibitory effect on NO and intracellular ROS generation. The cytotoxic effect of the purified peptide in EA.hy926 cells was assessed by MTT assay at multiple purified peptide concentrations (62.5, 125 and 250 μ M). No significant toxic effects were observed in the cells, which were treated with concentrations of up to 250 μ M of the purified peptide in the presence or absence of Ang II (Fig. 6A). Thus, based on this result, an NO production assay was performed at the peptide concentration of 250 μ M.

In order to determine whether the purified peptide inhibited the generation of Ang II-induced NO and intracellular ROS, which play central roles in endothelial dysfunction, the EA.hy926 cells were stimulated with Ang II in the absence or presence of the purified peptide. Ang II treatment alone markedly induced NO generation by the treated cells compared with the untreated cells. The purified peptide significantly inhibited NO generation by the Ang II-stimulated EA.hy926 cells (Fig. 6B). Subsequently, in order to confirm the inhibition of Ang II-induced oxidative stress in the EA.hy926 cells treated with the purified peptide, intracellular ROS generation was evaluated by monitoring DCFH-DA fluorescence (Fig. 7). The fluorescence intensity in the EA.hy926 cells increased markedly following exposure to Ang II compared with that in the untreated cells. Pre-treatment with the purified peptide inhibited the induction of increased fluorescence intensity induced by Ang II.

Effects of the purified peptide on endothelial dysfunction-related factors and the activation of mitogen-activated protein kinases (MAPKs) in Ang II-stimulated EA.hy926 cells. To examine the ability of the purified peptide to inhibit Ang II-mediated endothelial dysfunction, its effects on the expression of iNOS and ET-1 were determined in the presence of Ang II. In response to Ang II, the expression of iNOS and ET-1 was markedly increased, and the purified peptide inhibited the iNOS and ET-1 expression levels in a dose-dependent manner (Fig. 8). To elucidate the mechanisms of action of the purified peptide, we examined its effects on the phosphorylation of MAPKs in Ang II-stimulated endothelial cells. The levels of phosphorylated ERK, JNK and p38 MAPK were elevated in the EA.hy926 cells following treatment with Ang II alone. The purified peptide attenuated the Ang II-induced phosphorylation of p38 MAPK, but did not affect the phosphorylation of ERK and JNK (Fig. 9). These results suggested that the peptide inhibited the expression of iNOS and ET-1 by reducing the phosphorylation of p38 MAPK.

Discussion

Spirulina is one of the edible microalgae and contains a high amount of protein. It also contains all of the essential amino acids, which makes it a complete protein source (17). Thus, *Spirulina* is considered a useful material from which bioactive peptides can be obtained. Potent bioactive peptides have attracted attention in research that aims to promote human health and reduce disease risk (17). Bioactive peptides have previously been produced via the enzymatic hydrolysis of various bioresources that contain a high protein concentration (17,27). Simulated gastrointestinal digestion can be used as a production process for potent bioactive peptides, with the advantage that the obtained peptides will resist physiological digestion after oral intake (28). As previously reported, digestion by gastrointestinal proteases provides more potent bioactive peptides compared with those obtained using other types of enzyme digestions (29). Recently, a number of studies have found that specific bioactive peptides obtained from gastrointestinal hydrolysates have anti-hypertensive (30),

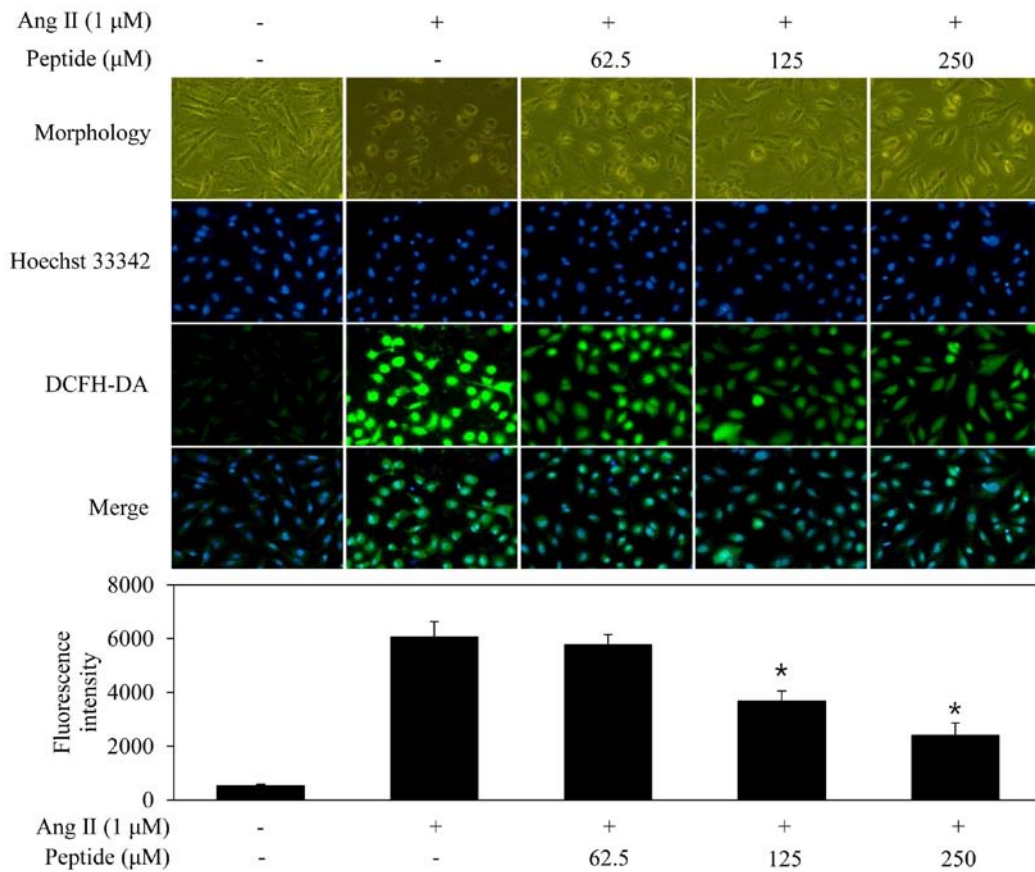


Figure 7. Inhibitory effects of peptide on angiotensin II (Ang II)-induced reactive oxygen species (ROS) generation in EA.hy926 cells. Cells were pre-treated with various concentrations of the purified peptide (62.5, 125 and 250 μ M) for 30 min, and then treated with Ang II for 30 min. The intracellular ROS generated was detected by 2',7'-dichlorodihydrofluorescein diacetate (DCFH-DA) assay. The values are expressed as the means \pm standard deviation of triplicate experiments. * p <0.05 indicate significant differences compared with the Ang II-stimulated group.

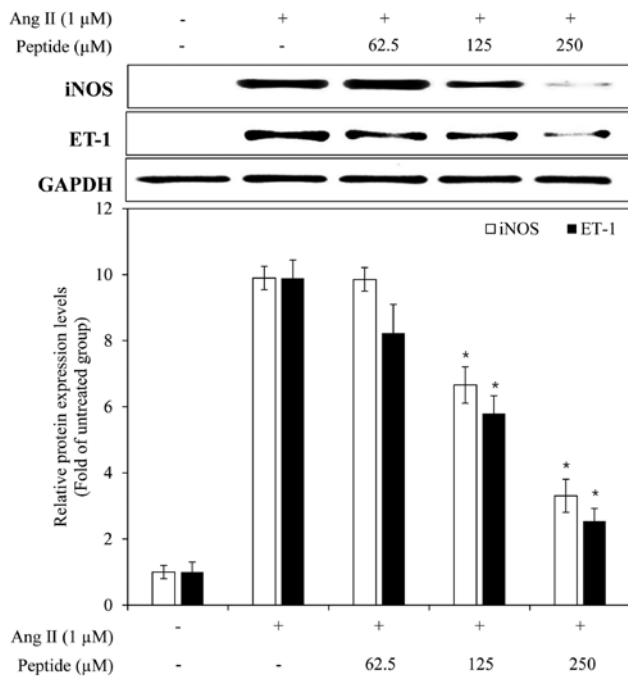


Figure 8. Inhibitory effect of the purified peptide on angiotensin II (Ang II)-induced inducible nitric oxide synthase (iNOS) and endothelin-1 (ET-1) in EA.hy926 endothelial cells. EA.hy926 cells were stimulated with Ang II for 24 h in the presence of the purified peptide (62.5, 125 and 250 μ M). The values are expressed as the means \pm standard deviation of triplicate experiments. * p <0.05 indicate significant differences compared with the Ang II-stimulated group.

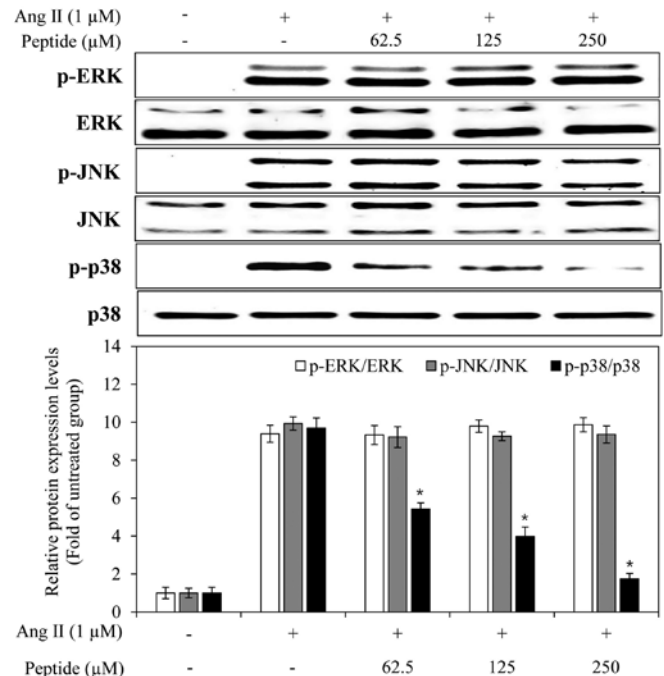


Figure 9. Inhibitory effect of the purified peptide on the protein level of mitogen activated protein kinases (MAPKs) in EA.hy926 endothelial cells. EA.hy926 cells were stimulated with angiotensin II (Ang II) for 30 min in the presence of the purified peptide (62.5, 125 and 250 μ M). The expression levels of MAPKs were determined by western blot analysis. The values are expressed as the means \pm standard deviation of triplicate experiments. * p <0.05 indicate significant differences compared with the Ang II-stimulated group.

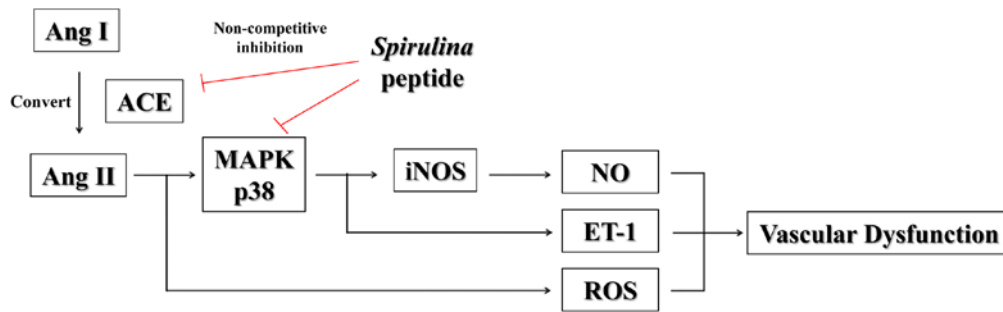


Figure 10. Summary of experimental results from the present study in the inhibition of angiotensin I (Ang I)-converting enzyme (ACE) and vascular dysfunction.

antioxidative (19), anticancer (31) and anti-inflammatory (32) effects. In the present study, we isolated an ACE inhibitory peptide from a gastrointestinal digest of *Spirulina* sp. protein, and the peptide was then investigated for its potential inhibitory effect on endothelial dysfunction in a human umbilical vein cell line.

Compared to a previous study, the ACE inhibitory activity of gastrointestinal hydrolysate from *Spirulina* sp. was more effective than that of gastrointestinal hydrolysate from silkworm pupa protein (33). Moreover, gastrointestinal hydrolysate of silkworm pupa protein was fractionated into 3 fractions (>10, 5-10 and <5 kDa) by UF according to molecular weights and the <5 kDa fraction exhibited strongest ACE inhibitory activity and similar with our results (33). Following purification, an ACE inhibitory peptide composed of 7 amino acids was obtained. According to previous findings, the inhibitory efficiency of ACE inhibitory peptides is highly influenced by their molecular weight and structure (6). Generally, ACE inhibitors contain structurally and functionally homologous features, such as dipeptidyl carboxypeptidase activity and zinc coordination geometry. Among ACE inhibitory peptides, the most potent and specific peptide inhibitors have similar structures, and ACE activity is strongly affected by the C-terminal tripeptide sequence of the substrate. The main substrates of peptide composition, such as Trp, Tyr, Phe, Pro and a hydrophobic amino acid at the C-terminal were found to be effective for ACE inhibitory activity due to the interaction among 3 sub-sites: S₁ (antepenultimate), S₁' (penultimate) and S₂' (ultimate), the active ACE site. In this study, the ACE inhibitory peptide obtained from a *Spirulina* sp. protein hydrolysate contained a Pro residue within its C-terminal tripeptide sequence, which may contribute to its ACE inhibitory activity. In addition, kinetic analysis by Lineweaver-Burk plots revealed that the purified peptide acts as a mixed non-competitive inhibitor. Moreover, based on molecular modeling, we were able to determine a mixed non-competitive inhibition mechanism of ACE by the purified peptide. This inhibition pattern type was similar to hard clam (34) and *Styela plicata* (35). Since the purified peptide does not share its binding site with Ang II, it does not compete for binding with the substrate. The peptide, however, binds in the cleft of the enzyme and next to the binding site of the substrate. The bound peptide may inhibit the conformational changes required to release Ang II, the end product, by forming about 6 hydrogen bonds with the enzyme. In addition, the purified peptide forms hydrogen

bonds with Ang II and holds it in the active site of the enzyme. Therefore, the peptide, enzyme, and Ang II form a dead-end complex, making it difficult for Ang II to leave the enzyme. Indeed, in this scenario, Ang II, the end product of catalysis by ACE, becomes a competitive inhibitor. Thus, the active site is occupied and another substrate cannot bind for the next enzymatic action.

In addition, the purified peptide also inhibited the Ang II-induced production of NO and intracellular ROS. Moreover, changes in cell morphology correlated with intracellular ROS production were recovered by treatment with the purified peptide. Ang II has been widely considered to be a systemic regulator of blood pressure (36). Moreover, it is known to be a strong vasoconstriction factor and a regulator of cardiac function (37). The excessive generation of intracellular ROS has been implicated in the pathogenesis of many cardiovascular diseases, including atherosclerosis, hypertension, heart failure and the associated endothelial dysfunction (38). According to a previous study, Ang II induces NO production via the expression of iNOS in the vascular smooth muscle cell (39). In addition, it does not affect the expression of endothelial nitric oxide synthase (eNOS) (40). Increased NO production via the expression of iNOS has been observed to trigger apoptotic and necrotic cell death in the neighboring tissue, for instance in atherosclerosis (41). ET-1 is another known vasoconstriction factor that, similar to Ang II, can induce endothelial dysfunction (42). Our results demonstrated that the purified ACE inhibitory peptide reduced the expression of iNOS and ET-1 in the Ang II-stimulated EA.hy926 cells.

MAPKs, including ERK, JNK and p38 kinase have been proposed to be activated in response to Ang II stimulation. According to previous studies, signaling by MAPKs promotes iNOS and ET-1 expression in Ang II-stimulated endothelial cells (43,44). In addition, the activation of MAPKs promotes the production of endothelial dysfunction-related factors in Ang II-stimulated endothelial cells (8). Thus, the inhibition of MAPK phosphorylation is a key mechanism. In the present study, we examined the effects of the purified ACE inhibitory peptide on the activation of MAPKs and found that the purified peptide attenuated the Ang II-induced phosphorylation of p38 MAPK.

In conclusion, we evaluated the effects of the ACE inhibitory peptide purified from a hydrolysate produced by the gastrointestinal digestion obtained from *Spirulina* sp. The ACE inhibitory pattern of the purified peptide was determined by Lineweaver-Burk plots and a mixed non-competitive inhibition

mechanism of this peptide was shown at the molecular level by molecular modeling. The purified peptide potently inhibited NO production, intracellular ROS, iNOS and ET-1 production and decreased the levels of phosphorylated p38 MAPK in Ang II-stimulated endothelial cells (Fig. 10). Consequently, it appears that this purified peptide has a beneficial effect on anti-hypertension and related diseases by inhibiting ACE and the cellular response to Ang II.

Acknowledgements

This study was supported by a grant from the Marine Biotechnology Program (20150220) funded by the Ministry of Oceans and Fisheries, Republic of Korea.

References

1. Yamada Y, Kato K, Yoshida T, Yokoi K, Matsuo H, Watanabe S, Ichihara S, Metoki N, Yoshida H, Satoh K, *et al.*: Association of polymorphisms of *ABCA1* and *ROS1* with hypertension in Japanese individuals. *Int J Mol Med* 21: 83-89, 2008.
2. Ko SC, Jung WK, Kang SM, Lee SH, Kang MC, Heo SJ, Kang KH, Kim YT, Park SJ, Jeong Y, *et al.*: Angiotensin I-converting enzyme (ACE) inhibition and nitric oxide (NO)-mediated antihypertensive effect of octaphloretol A isolated from *Ishige sinicola*: in vitro molecular mechanism and in vivo SHR model. *J Funct Foods* 18: 289-299, 2016.
3. Sanae M and Yasuo A: Green asparagus (*Asparagus officinalis*) prevented hypertension by an inhibitory effect on angiotensin-converting enzyme activity in the kidney of spontaneously hypertensive rats. *J Agric Food Chem* 61: 5520-5525, 2013.
4. Ahn CB, Jeon YJ, Kim YT and Je JY: Angiotensin I converting enzyme (ACE) inhibitory peptides from salmon byproduct protein hydrolysate by alcalase hydrolysis. *Process Biochem* 47: 2240-2245, 2012.
5. Tomita N, Yamasaki K, Izawa K, Kunugiza Y, Osako MK, Ogihara T and Morishita R: Improvement of organ damage by a non-depressor dose of imidapril in diabetic spontaneously hypertensive rats. *Int J Mol Med* 19: 571-579, 2007.
6. Ko SC, Kang N, Kim EA, Kang MC, Lee SH, Kang SM, Lee JB, Jeon BT, Kim SK, Park SJ, *et al.*: A novel angiotensin I-converting enzyme (ACE) inhibitory peptide from a marine *Chlorella ellipsoidea* and its antihypertensive effect in spontaneously hypertensive rats. *Process Biochem* 47: 2005-2011, 2012.
7. Qian ZJ, Je JY and Kim SK: Antihypertensive effect of angiotensin I converting enzyme-inhibitory peptide from hydrolysates of Bigeye tuna dark muscle, *Thunnus obesus*. *J Agric Food Chem* 55: 8398-8403, 2007.
8. Chen J, Li D, Schaefer R and Mehta JL: Cross-talk between dyslipidemia and renin-angiotensin system and the role of LOX-1 and MAPK in atherosclerosis studies with the combined use of rosuvastatin and candesartan. *Atherosclerosis* 184: 295-301, 2006.
9. Li JM and Shah AM: Mechanism of endothelial cell NADPH oxidase activation by angiotensin II. Role of the p47^{phox} subunit. *J Biol Chem* 278: 12094-12100, 2003.
10. Alonso-Galicia M, Maier KG, Greene AS, Cowley AW Jr and Roman RJ: Role of 20-hydroxyeicosatetraenoic acid in the renal and vasoconstrictor actions of angiotensin II. *Am J Physiol Regul Integr Comp Physiol* 283: R60-R68, 2002.
11. Gragasin FS, Xu Y, Arenas IA, Kainth N and Davidge ST: Estrogen reduces angiotensin II-induced nitric oxide synthase and NAD(P)H oxidase expression in endothelial cells. *Arterioscler Thromb Vasc Biol* 23: 38-44, 2003.
12. Hahn AW, Resink TJ, Scott-Burden T, Powell J, Dohi Y and Bühler FR: Stimulation of endothelin mRNA and secretion in rat vascular smooth muscle cells: a novel autocrine function. *Cell Regul* 1: 649-659, 1990.
13. Qian ZJ, Heo SJ, Oh CH, Kang DH, Jeong SH, Park WS, Choi IW, Jeon YJ and Jung WK: Angiotensin I-converting enzyme (ACE) inhibitory peptide isolated from biodiesel byproducts of marine microalgae, *Nannochloropsis oculata*. *J Biobased Mater Bioenergy* 7: 135-142, 2013.
14. Servaes K, Maesen M, Prandi B, Sforza S and Elst K: Polar lipid profile of *Nannochloropsis oculata* determined using a variety of lipid extraction procedures. *J Agric Food Chem* 63: 3931-3941, 2015.
15. Oh GW, Ko SC, Heo SY, Nguyen VT, Kim G, Jang CH, Park WS, Choi IW, Qian ZJ and Jung WK: A novel peptide purified from the fermented microalga *Pavlova lutheri* attenuates oxidative stress and melanogenesis in B16F10 melanoma cells. *Process Biochem* 50: 1318-1326, 2015.
16. Suetsuna K and Chen JR: Identification of antihypertensive peptides from peptic digest of two microalgae, *Chlorella vulgaris* and *Spirulina platensis*. *Mar Biotechnol (NY)* 3: 305-309, 2001.
17. Vo TS, Ryu B and Kim SK: Purification of novel anti-inflammatory peptides from enzymatic hydrolysate of the edible microalga *Spirulina maxima*. *J Funct Foods* 5: 1336-1346, 2013.
18. Samuels R, Mani UV, Iyer UM and Nayak US: Hypocholesterolemic effect of *Spirulina* in patients with hyperlipidemic nephrotic syndrome. *J Med Food* 5: 91-96, 2002.
19. Jung WK, Qian ZJ, Lee SH, Choi SY, Sung NJ, Byun HG and Kim SK: Free radical scavenging activity of a novel anti-oxidative peptide isolated from in vitro gastrointestinal digests of *Mytilus coruscus*. *J Med Food* 10: 197-202, 2007.
20. Cushman DW and Cheung HS: Spectrophotometric assay and properties of the angiotensin-converting enzyme of rabbit lung. *Biochem Pharmacol* 20: 1637-1648, 1971.
21. Bush K, Henry PR and Slusarchyk DS: Muraceins - muramyl peptides produced by *Nocardia orientalis* as angiotensin-converting enzyme inhibitors. I. Taxonomy, fermentation and biological properties. *J Antibiot (Tokyo)* 37: 330-335, 1984.
22. Raveh B, London N and Schueler-Furman O: Sub-angstrom modeling of complexes between flexible peptides and globular proteins. *Proteins* 78: 2029-2040, 2010.
23. Jorgensen WL, Chandrasekhar J, Madura JD, Impey RW and Klein ML: Comparison of simple potential functions for simulating liquid water. *J Chem Phys* 79: 926-935, 1983.
24. Phillips JC, Braun R, Wang W, Gumbart J, Tajkhorshid E, Villa E, Chipot C, Skeel RD, Kalé L and Schulten K: Scalable molecular dynamics with NAMD. *J Comput Chem* 26: 1781-1802, 2005.
25. MacKerell AD Jr, Bashford D, Bellott M, Dunbrack RL Jr, Evanseck JD, Field MJ, Fischer S, Gao J, Guo H, Ha S, *et al.*: All-atom empirical potential for molecular modeling and dynamics studies of proteins. *J Phys Chem B* 102: 3586-3616, 1998.
26. Toukmaji A, Sagui C, Board J and Darden T: Efficient particle-mesh Ewald based approach to fixed and induced dipolar interactions. *J Chem Phys* 113: 10913-10927, 2000.
27. Ko SC, Lee JK, Byun HG, Lee SC and Jeon YJ: Purification and characterization of angiotensin I-converting enzyme inhibitory peptide from enzymatic hydrolysates of *Styela clava* flesh tissue. *Process Biochem* 47: 34-40, 2012.
28. Qian ZJ, Jung WK, Byun HG and Kim SK: Protective effect of an antioxidative peptide purified from gastrointestinal digests of oyster, *Crassostrea gigas* against free radical induced DNA damage. *Bioresour Technol* 99: 3365-3371, 2008.
29. Himaya SWA, Ngo DH, Ryu B and Kim SK: An active peptide purified from gastrointestinal enzyme hydrolysate of Pacific cod skin gelatin attenuates angiotensin-I converting enzyme (ACE) activity and cellular oxidative stress. *Food Chem* 132: 1872-1882, 2012.
30. Jung WK, Mendis E, Je JY, Park PJ, Son BW, Kim HC, Choi YK and Kim SK: Angiotensin I-converting enzyme inhibitory peptide from yellow sole (*Limanda aspera*) frame protein and its antihypertensive effect in spontaneously hypertensive rats. *Food Chem* 94: 26-32, 2006.
31. Nguyen VT, Qian ZJ, Ryu B, Kim KN, Kim D, Kim YM, Jeon YJ, Park WS, Choi IW, Kim GH, *et al.*: Matrix metalloproteinases (MMPs) inhibitory effects of an octameric oligopeptide isolated from abalone *Haliotis discus hannai*. *Food Chem* 141: 503-509, 2013.
32. Qian ZJ, Ryu B, Park WS, Choi IW and Jung WK: Inhibitory effects and molecular mechanism of an anti-inflammatory peptide isolated from intestine of abalone, *Haliotis discus hannai* on LPS-induced cytokine production via the p-38/p-JNK pathways in RAW264.7 macrophages. *J Food Biochem* 4: 690-698, 2016.
33. Wu Q, Jia J, Yan H, Du J and Gui Z: A novel angiotensin-I converting enzyme (ACE) inhibitory peptide from gastrointestinal protease hydrolysate of silkworm pupa (*Bombyx mori*) protein: biochemical characterization and molecular docking study. *Peptides* 68: 17-24, 2015.
34. Tsai JS, Chen JL and Pan BS: ACE-inhibitory peptides identified from the muscle protein hydrolysate of hard clam (*Meretrix lusoria*). *Process Biochem* 43: 743-747, 2008.
35. Ko SC, Kang MC, Lee JK, Byun HG, Kim SK, Lee SC, Jeon BT, Park PJ, Jung WK and Jeon YJ: Effect of angiotensin I-converting enzyme (ACE) inhibitory peptide purified from enzymatic hydrolysates of *Styela plicata*. *Eur Food Res Technol* 233: 915-922, 2011.

36. Griendling KK, Murphy TJ and Alexander RW: Molecular biology of the renin-angiotensin system. *Circulation* 87: 1816-1828, 1993.
37. Kagiya S, Eguchi S, Frank GD, Inagami T, Zhang YC and Phillips MI: Angiotensin II-induced cardiac hypertrophy and hypertension are attenuated by epidermal growth factor receptor antisense. *Circulation* 106: 909-912, 2002.
38. Cai H and Harrison DG: Endothelial dysfunction in cardiovascular diseases: the role of oxidant stress. *Circ Res* 87: 840-844, 2000.
39. Millatt LJ, Abdel-Rahman EM and Siragy HM: Angiotensin II and nitric oxide: a question of balance. *Regul Pept* 81: 1-10, 1999.
40. Olson SC, Dowds TA, Pino PA, Barry MT and Burke-Wolin T: ANG II stimulates endothelial nitric oxide synthase expression in bovine pulmonary artery endothelium. *Am J Physiol* 273: L315-L321, 1997.
41. Hemmrich K, Suschek CV, Lerzynski G and Kolb-Bachofen V: iNOS activity is essential for endothelial stress gene expression protecting against oxidative damage. *J Appl Physiol* 95: 1937-1946, 2003.
42. Ito H, Hirata Y, Adachi S, Tanaka M, Tsujino M, Koike A, Nogami A, Murumo F and Hiroe M: Endothelin-1 is an autocrine/paracrine factor in the mechanism of angiotensin II-induced hypertrophy in cultured rat cardiomyocytes. *J Clin Invest* 92: 398-403, 1993.
43. Jung WK, Choi I, Lee DY, Yea SS, Choi YH, Kim MM, Park SG, Seo SK, Lee SW and Lee CM: Caffeic acid phenethyl ester protects mice from lethal endotoxin shock and inhibits lipopolysaccharide-induced cyclooxygenase-2 and inducible nitric oxide synthase expression in RAW 264.7 macrophages via the p38/ERK and NF-kappaB pathways. *Int J Biochem Cell Biol* 40: 2572-2582, 2008.
44. Kyaw M, Yoshizumi M, Tsuchiya K, Kirima K, Suzuki Y, Abe S, Hasegawa T and Tamaki T: Antioxidants inhibit endothelin-1 (1-31)-induced proliferation of vascular smooth muscle cells via the inhibition of mitogen-activated protein (MAP) kinase and activator protein-1 (AP-1). *Biochem Pharmacol* 64: 1521-1531, 2002.